3D Embryogenesis Image Segmentation by the Generalized Subjective Surfaces Method using the Finite Volume Technique

K. Mikula, N. Peyriéras, M. Remešíková, A. Sarti

Department of Mathematics, Slovak University of Technology, Radlinského 11, 81368 Bratislava, Slovakia, mikula@math.sk, remesik@math.sk

CNRS-DEPSN, Institut de Neurobiologie Alfred Fessard, Avenue de la Terrasse, 91198 Gif sur Yvette, France, nadine.peyrieras@iaf.cnrs-gif.fr

DEIS, University of Bologna, Bologna, Italy, asarti@deis.unibo.it

ABSTRACT. *In this paper, an efficient finite volume method for image segmentation is introduced. The method is based on surface evolution governed by a nonlinear PDE, the generalized subjective surfaces equation. Our numerical method is based on semi-implicit time discretization and finite volume space approximation. We show examples of image segmentation - particularly, we deal with images of early embryogenesis of zebrafish obtained by a confocal microscope. We mention how the segmentation can be useful for analysis of the embryo images and reconstruction of the embryo evolution.*

KEYWORDS: *image segmentation, surface evolution, subjective surfaces method, semi-implicit scheme finite volume method, embryogenesis*

1. Introduction

Embryogenesis, the process of embryo evolution, is nowadays one of the main topics for biomedical research. Even from the very beginning, the process is quite complex as it contains cell divisions, movement and deformation, differentiation and interactions. Modern technical equipment allows us to make 3D images of embryos in short time intervals and thus to observe the process of evolution and possibly track each particular cell in time. In this paper we process long time sequences of 3D images of a zebrafish (Danio Rerio) embryo obtained by a confocal microscope.

Obtaining the images by microscope is the first step of the research. Next, in order to obtain some useful information, various image processing techniques have to be applied. The image segmentation is necessary to extract the particular cell from the

image and analyze its size and shape. It can be also used for quantitative analysis of the embryo – counting the number of cells in the image, determining the volume of the embryo and the density of cells in the organism. Finally, we can use it for finding correspondences between cells in subsequent time steps and for detecting some significant cell behavior, for example mitosis (division). In spite of quickly developing technical equipment, it is still hard to obtain images suitable for embryo analysis. The images usually suffer from some noise, the borders of cells might be unclear or corrupted, and there can be some artifacts in the image. Also, it is necessary to analyze a large quantity of images and each one of them can contain thousands of cells. All this makes strong demands on the segmentation method: it has to be fast, stable and precise, able to detect objects with incomplete borders and operate in noisy images.

The main goal of this paper is to introduce an efficient method for 3D image segmentation. The method is obtained by generalizing the subjective surfaces method [SMSETHIAN1], which was previously proved to work very well for non-trivial images and practical applications [CMSSG, FMPS, SMSETHIAN1]. The generalization lies in considering the classical model equation in a convection-diffusion form and then using different weights for the convection and the diffusion terms. We will show that it speeds up the segmentation process. Our numerical method is based on the semi-implicit time discretization of nonlinear diffusion [HMSG1] and the flux based finite volume technique for the space approximation [FM1]. As the image intensity can be seen as a piecewise constant function (constant for each voxel), it appears to be the natural choice. Study of the experimental order of convergence also shows that the method converges to true solution of the segmentation equation.

2. The generalized subjective surface method

The subjective surfaces method is based on surface evolution. At the beginning, we take a function (called segmentation function) and we let it evolve so that its isosurfaces are taking the shape of the segmented object. The evolution is driven by the image intensity function, more precisely by the position of edges in the image. Ideally, the process ends up with a function whose isosurfaces all have the shape of the object that we want to extract.

The so-called geodesic mean curvature flow equation was introduced to image segmentation in [CKS, KKOTY]

$$\partial_t u = |\nabla u| \nabla . \left(g(|\nabla I_\sigma|) \frac{\nabla u}{|\nabla u|} \right) = \nabla g . \nabla u + g\, |\nabla u| \nabla . \left(\frac{\nabla u}{|\nabla u|} \right) . \qquad [1]$$

There, the authors followed one particular level set of u to segment the object in the image. Changing the view from one level set approach to a more robust graph evolution, and using Evans-Spruck type regularization, $|\nabla u| \approx \sqrt{\varepsilon^2 + |\nabla u|^2}$, we obtain the classical subjective surface equation [SMSETHIAN1]

$$\partial_t u = \sqrt{\varepsilon^2 + |\nabla u|^2} \nabla . \left(g(|\nabla I_\sigma|) \frac{\nabla u}{\sqrt{\varepsilon^2 + |\nabla u|^2}} \right) , \qquad [2]$$

where $u(\mathbf{x}, t)$ is the segmentation function. By I_σ we denote $G_\sigma * I_0$, i.e. convolution of $I_0(\mathbf{x})$ – the intensity of the original image – with the heat kernel. The function $g(s)$ is called the edge detector function. According to [CKS, KKOTY, SMSETHIAN1] we use $g(s) = 1/(1 + Ks^2)$, where K is a positive constant. We can see that the edge detector function gives small values for large gradients in the (convolved) image. It also has an important property that $-\nabla g$ points towards the edges in the image. Generally, we can also use $g(s) = f(1/(1 + Ks^2))$ which can, for a suitably chosen function f, speed up the process and improve the quality of the results. In some cases, additional smoothing of $g(s)$ by convolution can be useful as well. Of course, modification has to be chosen so that the above mentioned important properties of edge detector are preserved.

Similarly to [Z], we can generalize [2] by introducing new coefficients w_{con} and w_{dif} that represent weights for the convection and the diffusion terms in its advection-diffusion form, cf. [1]. The new model reads:

$$\partial_t u = w_{con} \nabla g . \nabla u + w_{dif} g \sqrt{\varepsilon^2 + |\nabla u|^2} \nabla . \frac{\nabla u}{\sqrt{\varepsilon^2 + |\nabla u|^2}} \,. \qquad [3]$$

Introducing new parameters in the equation, the model becomes more flexible. Having the possibility to control separately the convective and diffusive processes, we have the potential to improve the efficiency of the method. We solve the problem in the domain $\Omega \times [0, T]$ and use the following boundary and initial conditions:

$$u(\mathbf{x}, t) = 0 \,, \quad \mathbf{x} \in \partial\Omega \,, \qquad u(\mathbf{x}, 0) = u_0(\mathbf{x}) \,. \qquad [4]$$

3. Numerical approximation

3.1. *Semi-implicit time discretization*

First, we discretize [3] in time. For this purpose, we use semi-implicit time discretization that leads to the following equation for $n = 1 \ldots N$, $\tau = T/N$:

$$\frac{u^n - u^{n-1}}{\tau} - w_{con} \nabla g . \nabla u^{n-1} = w_{dif} g \sqrt{\varepsilon^2 + |\nabla u^{n-1}|^2} \nabla . \frac{\nabla u^n}{\sqrt{\varepsilon^2 + |\nabla u^{n-1}|^2}} . \quad [5]$$

Applying this technique makes the method unconditionally stable for the diffusion part, and the time step is limited only by the CFL condition related to convection.

3.2. *Finite volume space discretization*

In order to discretize [5] in space, we use the finite volume strategy. We identify the finite volume mesh $\mathcal{T}_h$ with the voxels of 3D image and denote each finite volume by V_{ijk}, $i = 1 \ldots N_1$, $j = 1 \ldots N_2$, $k = 1 \ldots N_3$. For each $V_{ijk} \in \mathcal{T}_h$ let N_{ijk} denote

the neighbors index shift, i.e., the set of all (p,q,r), such that $p,q,r \in \{-1,0,1\}$, $|p|+|q|+|r|=1$. Let $m(V_{ijk})$ denote the volume of V_{ijk}. The line connecting the center of V_{ijk} and the center of its neighbor $V_{i+p,j+q,k+r}$, $(p,q,r) \in N_{ijk}$ is denoted by σ_{ijk}^{pqr} and its length $m(\sigma_{ijk}^{pqr})$. Our finite volume grid being regular rectangular, let h_1, h_2, h_3 represent the size of finite volumes in x_1, x_2, x_3 direction, respectively. The planar sides of finite volume V_{ijk} are denoted by e_{ijk}^{pqr} with area $m(e_{ijk}^{pqr})$ and normal ν_{ijk}^{pqr}. Let x_{ijk}^{pqr} be the point where the line σ_{ijk}^{pqr} crosses the side e_{ijk}^{pqr}. Integrating [5] over every finite volume V_{ijk}, we get

$$\int_{V_{ijk}} \frac{u^n - u^{n-1}}{\tau} d\mathbf{x} - \int_{V_{ijk}} w_{con} \nabla g . \nabla u^{n-1} d\mathbf{x} = \qquad [6]$$
$$\int_{V_{ijk}} w_{dif} g \sqrt{\varepsilon^2 + |\nabla u^{n-1}|^2} \nabla . \frac{\nabla u^n}{\sqrt{\varepsilon^2 + |\nabla u^{n-1}|^2}} d\mathbf{x} = 0\,.$$

As u^n, u^{n-1} are piecewise constant, we can rewrite the first term on the LHS:

$$\int_{V_{ijk}} \frac{u^n - u^{n-1}}{\tau} d\mathbf{x} = m(V_{ijk}) \frac{u_{ijk}^n - u_{ijk}^{n-1}}{\tau}\,. \qquad [7]$$

In order to approximate other terms, we have to perform several steps. First, the term $|\nabla u^{n-1}|$, resp. $|\nabla I_\sigma|$, occurs in the integrals and we will need to approximate the average modulus of these terms in both V_{ijk} and on voxel sides e_{ijk}^{pqr}. Let us use the following definitions for $p,q,r \in N_{ijk}$:

$$\begin{aligned}
\nabla^{p00} u_{ijk}^n &= (p(u_{i+p,j,k}^n - u_{ijk}^n)/h_1, (u_{ijk}^{p10} - u_{ijk}^{p,-1,0})/h_2, (u_{ijk}^{p01} - u_{ijk}^{p,0,-1})/h_3) \\
\nabla^{0q0} u_{ijk}^n &= ((u_{ijk}^{1q0} - u_{ijk}^{-1,q,0})/h_1, q(u_{i,j+q,k}^n - u_{ijk}^n)/h_2, (u_{ijk}^{0q1} - u_{ijk}^{0,q,-1})/h_3) \\
\nabla^{00r} u_{ijk}^n &= ((u_{ijk}^{10r} - u_{ijk}^{-1,0,r})/h_1, (u_{ijk}^{01r} - u_{ijk}^{0,-1,r})/h_2, r(u_{i,j,k+r}^n - u_{ijk}^n)/h_3) \\
u_{ijk}^{pq0} &= \frac{1}{4}(u_{ijk}^n + u_{i+p,j,k}^n + u_{i,j+q,k}^n + u_{i+p,j+q,k}^n) \\
u_{ijk}^{p0r} &= \frac{1}{4}(u_{ijk}^n + u_{i+p,j,k}^n + u_{i,j,k+r}^n + u_{i+p,j,k+r}^n) \\
u_{ijk}^{0qr} &= \frac{1}{4}(u_{ijk}^n + u_{i,j+q,k}^n + u_{i,j,k+r}^n + u_{i,j+q,k+r}^n).
\end{aligned}$$

These formulas can be understood as an approximation of the gradient in the point x_{ijk}^{pqr}, a barycenter of e_{ijk}^{pqr}. Now we define

$$Q_{ijk}^{pqr;n-1} = \sqrt{\varepsilon^2 + |\nabla^{pqr} u_{ijk}^{n-1}|^2},\ \ \overline{Q}_{ijk}^{n-1} = \sqrt{\varepsilon^2 + \frac{1}{6} \sum_{N_{ijk}} |\nabla^{pqr} u_{ijk}^{n-1}|^2}$$

and $g_{ijk} = g(\frac{1}{6}\sum_{N_{ijk}} |\nabla^{pqr} I_{\sigma;ijk}|)$. Moreover, let us denote $v = -w_{con}\nabla g$. As suggested in [FM1], the convective term can be written in the equivalent form $v.\nabla u^{n-1} = \nabla.(vu^{n-1}) - u^{n-1}\nabla.v$ and therefore, considering u^{n-1} constant in V_{ijk} we get

$$\int_{V_{ijk}} v.\nabla u^{n-1} \quad = \quad \sum_{N_{ijk}} \int_{e^{pqr}_{ijk}} u^{n-1} v.\nu^{pqr}_{ijk}\, d\gamma + u^{n-1}_{ijk} \sum_{N_{ijk}} \int_{e^{pqr}_{ijk}} v.\nu^{pqr}_{ijk}\, d\gamma. \quad [8]$$

Let us define

$$v^{pqr}_{ijk} = m(e^{pqr}_{ijk}) \left(-w_{con} \frac{g_{i+p,j+q,k+r} - g_{ijk}}{m(\sigma^{pqr}_{ijk})} \right),$$

where we consider the approximation of $\nabla g.\nu^{pqr}_{ijk}$. We will distinguish between the outflow and inflow boundaries by defining two sets of indices $N^{out}_{ijk} = \{(p,q,r) \in N_{ijk}\,,\, v^{pqr}_{ijk} > 0\}\,, \quad N^{in}_{ijk} := \{(p,q,r) \in N_{ijk}\,,\, v^{pqr}_{ijk} \leq 0\}\,.$ If we use the upwind principle for approximating the first integral on the RHS in [8], we obtain

$$\begin{aligned} \int_{V_{ijk}} v.\nabla u^{n-1} \quad &\approx \quad \sum_{N^{out}_{ijk}} u^{n-1}_{ijk} v^{pqr}_{ijk} + \sum_{N^{in}_{ijk}} u^{n-1}_{i+p,j+q,k+r} v^{pqr}_{ijk} - u^{n-1}_{ijk} \sum_{N_{ijk}} v^{pqr}_{ijk} \\ &= \quad \sum_{N^{in}_{ijk}} (u^{n-1}_{i+p,j+q,k+r} - u^{n-1}_{ijk}) v^{pqr}_{ijk}\,. \end{aligned} \quad [9]$$

The diffusion part can be discretized in a very similar way. We can write

$$\begin{aligned} &\int_{V_{ijk}} w_{dif}\, g \sqrt{\varepsilon^2 + |\nabla u^{n-1}|^2} \nabla. \frac{\nabla u^n}{\sqrt{\varepsilon^2 + |\nabla u^{n-1}|^2}} d\mathbf{x} \approx \\ &w_{dif}\; g_{ijk}\; \bar{Q}^{n-1}_{ijk} \sum_{|p|+|q|+|r|=1} \int_{e^{pqr}_{ijk}} \frac{\nabla u^n}{\sqrt{\varepsilon^2 + |\nabla u^{n-1}|}} .\nu^{pqr}_{ijk}\, d\gamma \approx \\ &w_{dif}\; g_{ijk}\; \bar{Q}^{n-1}_{ijk} \sum_{|p|+|q|+|r|=1} m(e^{pqr}_{ijk}) \frac{u^n_{i+p,j+q,k+r} - u^n_{ijk}}{Q^{pqr;n-1}_{ijk} m(\sigma^{pqr}_{ijk})}\,. \end{aligned} \quad [10]$$

Finally, putting together [7], [9], [10] and boundary conditions, we obtain a linear system with unknowns u^n_{ijk}. We solve it by the successive over relaxation (SOR) method. Since we start the iterative process using the result from the previous time step, the SOR method is sufficiently fast.

3.3. *Experimental order of convergence of the numerical scheme*

In order to experimentally verify the convergence of the method, we compute the experimental order of convergence (EOC) for a test case. Since no analytical solution is known for this highly nonlinear problem, we put function $\tilde{u}(x,y,z,t) = tcos(\pi x)cos(\pi y)cos(\pi z)$, fulfilling [4], into the equation. Then we get a problem

with a given right hand side and modify our scheme accordingly. As the edge indicator we take function $g(x,y,z) = cos^2(\pi x)cos^2(\pi y)cos^2(\pi z)$, the model parameters $w_{con} = 1$,$w_{dif} = 1$, $\varepsilon = 10^{-6}$, $\Omega = [-0.5, 0.5]^3$, $T = 0.1$, and we consider relation $\tau = h^2$ which is standard when testing EOC for problems with the diffusion term. Table 3.3 shows the values of error in $L_2((0,T), L_2(\Omega))$ norm for subsequently refined grids. We can see that the method converges with an order bigger than 1.

h	τ	$L_2((0,T), L_2(\Omega)) - error$	EOC
0.1	0.01	0.013657	
0.05	0.0025	0.007088	0.94619
0.025	0.000625	0.003103	1.19171
0.0125	0.00015625	0.001256	1.30482
0.00625	0.0000390625	0.000495	1.34333

Table 1. *Experimental order of convergence for a test case*

4. Segmentation results

Now we will illustrate how the method can be used in biomedical applications. We deal with a time sequence (700 time steps) of 3D images of zebrafish embryo. The dimensions of each image are $512 \times 512 \times 74$ voxels. There are two types of images: cell nuclei and cell membranes.

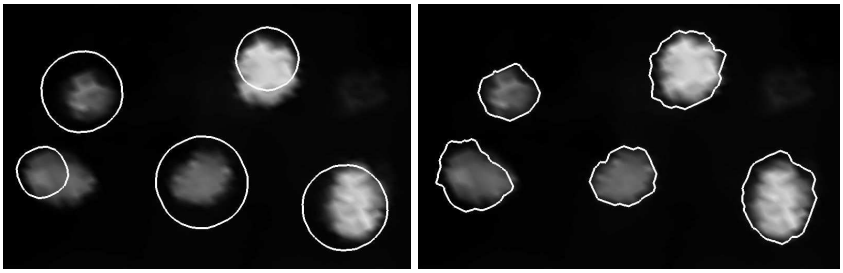

Figure 1. *Segmentation of cell nuclei. On the left, the initial forms of segmentation functions. On the right, the results of segmentation*

First we segment the nuclei images, each nucleus individually. To initialize the segmentation function, we consider that the nuclei have shapes similar to a sphere or ellipsoid, so we use function that has all isosurfaces identical and of the shape of an ellipsoid. The centers of the ellipsoids are given by the estimated centers of cell nuclei given by the method introduced in [FMPS]. The radii of the ellipsoids are chosen by estimating the size of the cell, based on measuring the distance from its nearest neighbor. The model parameters are chosen as follows: $g(s) = G_\rho * \frac{1}{(1+Ks^2)^6}$, $K = 1000$, $\rho = 0.1$, $w_{con} = 10.0$, $w_{dif} = 2.0$. Time step $\tau = 0.1$ and space step $h = 1.0$. The results can be seen in Figure 1. In all figures in this section, we display a planar cut of the embryo (x-y plane) or its clip. We show isosurface $u = 127$ of the

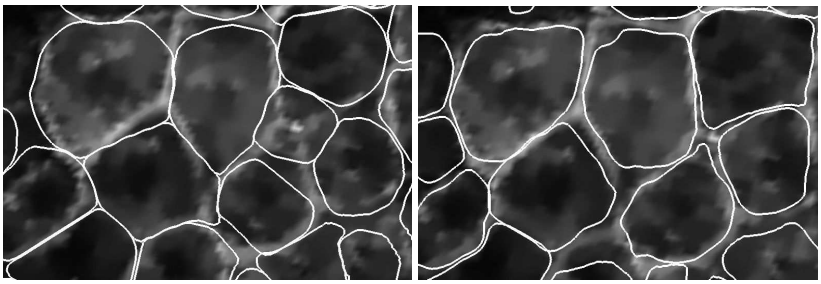

Figure 2. *Segmentation of cell membranes. On the left, the initial forms of segmentation functions. On the right, the results of segmentation*

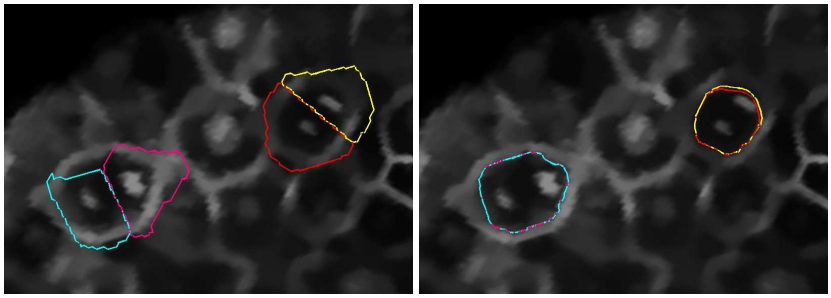

Figure 3. *Detection of mitoses. On the left, we can see the initial forms of segmentation functions. On the right, the results of segmentation indicates that the two centers (nuclei) belong to one cell.*

initial and final segmentation function. Let us note that segmentation of one nucleus took about 5 seconds in average, and it appears to be about 10 times faster than the segmentation by the classical subjective surfaces method [CMSSG, SMSETHIAN1] or by the segmentation using explicit finite difference schemes [Z].

As for the segmentation of membrane images, the initial form of segmentation function is of 'Voronoi' type. We start from an ellipsoid situated in the cell center as in the case of nuclei, but when some point inside the ellipsoid belongs to an ellipsoid of another cell, the function there is set to zero. The edge detector $g(s) = \frac{1}{1+Ks^2}$, $K = 1000$, $w_{con} = 10.0$, $w_{dif} = 0.2$, $\tau = 0.1$ and $h = 1.0$. We can see an example in Figure 2. Again, the method appeared to be faster than the classical method or the explicit finite difference scheme.

The membrane segmentation has an interesting application – it can be used for mitosis detection. Possible mitosis can be detected as a situation when there are two nuclei in one cell. When membrane segmentation gives approximately the same result when started from two different centers, this means that the two centers (nuclei) belong to the same cell and the cell can be marked as a candidate for mitosis, see Figure 3.

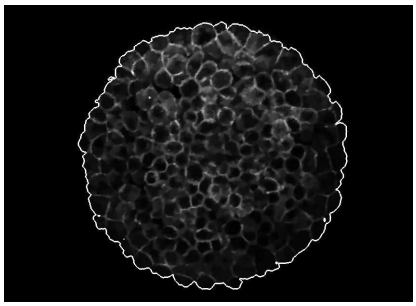

Figure 4. *Segmentation of whole embryo*

Finally, using the membrane image, we can segment the whole embryo, see Figure 4. Then we can determine the volume of the embryo and the density of cells in it, and consequently the time evolution of these quantities, which has an impact in biology.

Acknowledgement

This work was supported by the grants VEGA 1/3321/06, APVT-RPEU-0004-06 and European projects Embryomics and BioEmergences.

5. Bibliography

[1] CASELLES V., KIMMEL R., SAPIRO G.,"Geodesic active contours" *Int. J. Comput. Vis*, vol. 22, p. 61-79, 1997.

[2] CORSARO S., MIKULA K., SARTI A., SGALLARI F.,"Semi-implicit co-volume method in 3D image segmentation", *SIAM J. Sci. Comput.*, vol. 28, num. 6, p. 2248-2265, 2006.

[3] FROLKOVIČ P., MIKULA K.,"Flux-based level set method: A finite volume method for evolving interfaces", *Applied Numerical Mathematics*, vol. 57, num. 4, p. 436-454, 2007.

[4] FROLKOVIČ P., MIKULA K., PEYRIÉRAS N., SARTI A.,"A counting number of cells and cell segmentation using advection-diffusion equations", *Kybernetika*, vol. 43, num. 6, p. 817-829, 2007.

[5] HANDLOVIČOVÁ A., MIKULA K., SGALLARI F., "Semi-implicit complementary volume scheme for solving level set like equations in image processing and curve evolution", *Numer. Math.*, vol. 93, p. 675-695, 2003.

[6] KICHENASSAMY S., KUMAR A., OLVER P., TANNENBAUM A., YEZZI A., "Conformal curvature flows: From phase transitions to active vision" *Arch. Rat. Mech. Anal.*, vol. 134 p. 275-301, 1996.

[7] SARTI A., MALLADI R., SETHIAN J.A.,"Subjective Surfaces: A Method for Completing Missing Boundaries", *PNAS*, vol. 12 num. 97, p. 6258-6263, 2000.

[8] ZANELLA C., CAMPANA M, MELANI C, RIZZI B., BOURGINE P., MIKULA K., PEYRIÉRAS N., SARTI A.,"Cells segmentation from 3D+time confocal images of early zebrafish embryogenesis", *Conf. Proc. IEEE Eng. Med. Biol. Soc.*, vol. 1, p. 1631-4, 2007.